Journal of the Egyptian Society of Parasitology, Vol. 54, No. 2, August 2024
J. Egypt. Soc. Parasitol. (JESP), 54(2), 2024: 325 - 334
Online: 2090-2549

THERAPEUTIC EFFECT OF ARTEMISIA ABSINTHIUM AND CURCUMA LONGA COMBINATION AGAINST CRYPTOSPORIDIOSIS IN IMMUNO-SUPPRESSED MURINE MODEL

By
NORAN M. ELDAWY[1], AZZA SAAD ELGHAREEB[2], HEBA E. ABDEL AATY[3], IBRAHIM ALY[4] and NANCY O. KAMEL[2]

[1]Department of Medical Parasitology, Faculty of Medicine - Misr University for Science and Technology, [2]Department of Medical Parasitology, Faculty of Medicine- October 6 University, [3]Department of Medical Parasitology, Faculty of Medicine- Ain Shams University, 11566 Cairo and Armed Forces College of Medicine (AFCM), 11774 Cairo, [4]Department of Medical Parasitology, Theodore Bilharz Research Institute, Giza, Egypt (*Correspondence: noran.mostafa@must.edu.eg)

Abstract

Infection by *Cryptosporidium* species causing cryptosporidiosis is considered a life-threatening condition in immunosuppressed patients, with unfortunately limited treatment options. This study evaluated the efficacy of *Artemisia absinthium* (AA) and *Curcuma longa* (CL) combination therapy unloaded and loaded on chitosan nanoparticles (CS NPs) and conjugated with conventional nitazo- xanide (NTZ) in treating cryptosporidiosis in immunosuppressed mice. The study design included fifty-six immunosuppressed mice classified into three main groups, divided into subgroups; eight mice each: GIA: non-infected non-treated, GIB: infected non-treated, GII: infected and treated with: CS NPs conventional free NTZ (GIIIA), AA and CL loaded on Cs NPs (GIIIB), conjugated AA and CL with NTZ loaded on Cs NPs (GIIIC), and AA and CL free combination (GIIID). Treatment efficacy was evaluated via parasitological examination, histopathological parameters, and the determination of oxidative stress markers. The most significant results were in the immun- osuppressed mice received unloaded unconjugated AA and CL free combination (GIIID) with a highly significant reduction (88%) in *C. parvum* oocysts shedding. Also, a remarked histo-patholo- gical improvement was revealed in the intestinal tissue sections nearly back to normal architecture and to lesser extent in extra-intestinal tissue sections in the same treated group. Meanwhile, oxidative stress markers (GSH & MDA) levels showed a high significant improvement ($P< 0.001$) in GIIID versus other treated ones.

Keywords: Mice, cryptosporidiosis, immunosuppressed, nitazoxanide, *Artemisia absinthium*, *Cur-cuma longa*, nanoparticles, CS NPs.

Introduction

Cryptosporidium parvum is an intracellular gastrointestinal coccidian zoonotic protozoon of medical importance that infects a wide range of humans and animals worldwide (Henin, 2022). The highest prevalence of cryptosporidiosis was detected in developing countries with a high mortality rate in children below the age of two years old (Bouzid *et al*, 2018). It was considered a serious, life-threatening public health problem in immunocompromised and immune-deficient cases, such as those with acquired immunodeficiency syndrome (AIDS) and patients receiving immunosuppressant drugs (Breurec *et al*, 2016). The parasite is mainly restricted to the intestinal tract; however, in immuno-compromised hosts, the biliary tract, liver, pancreas, lungs, and probably other organs may also be infected (McCole *et al*, 2000).

The most common drug that was approved by the FDA to treat *C. parvum* infection is nitazoxanide (NTZ) as a broad-spectrum antiparasitic drug (Checkley *et al*, 2015; Henin, 2022). However, it was not effective in immunocompromised and malnourished patients, which raises the need for effective and safe alternatives (Moawad *et al*, 2021).

In the last decade, various herbal products showed unique pharmacological activity against a wide range of infectious agents, including parasites (Khater *et al*, 2017; Soufy *et al*, 2017). Herbal *Artemisia spp.* (mugworts) and *Curcuma longa* (curcumin) were

proved to be promising in the treatment of helminthic and protozoal infections (Ferreira *et al*, 2011; Asadpour *et al*, 2018; Beshay, 2018; Ekiert *et al*, 2021). *Artemisia* spp., *Artemisia absinthium,* and *Artemisia annua* are also herbs that were used as antiparasitic agents. The two species was referred to as a wormwood because of their anthelminthic effect known since the ancient Egyptians (Padosch *et al*, 2006). *Artemisia* antiparasitic effect was proved by several experimental studies were used against *Trichinella spiralis* (Caner *et al*, 2008), *Fasciola hepatica*, *Schistosoma mansoni*, *Hymenolepis nana*, *Plasmodium falciparum*, and *Cryptosporidium parvum* (El-Ashkar *et al*, 2022). Curcumin is considered a cheap and safe herb, with rare or no toxicity even in high concentrations, which made it a perfect choice for treating immunocompromised cases (Nanjwade *et al*, 2015).

Also, nanotechnology and nanoparticle carrier molecules have attracted a lot of interest in the medical field (De Jong and Borm, 2008). One of the most important natural and low-cost nanoparticles (NPs) is chitosan (CS), which could be obtained on large scale from crustacean shells, the cuticle of insects, and the cell wall of fungi. CS was considered a NP of choice due to its significant properties as being a natural product expected to be of low toxicity (Yanat and Schroen, 2021).

This study aimed to assess the efficacy of the free combination of *Artemisia absinthium* and *Curcuma longa* or loaded on chitosan nanoparticles, and conjugated with the conventional nitazoxanide in the treatment of cryptosporidiosis model in immunosuppressed mice.

Material and methods

Experimental animals: The study was carried out on 56 immunosuppressed laboratory-bred male Swiss Albino mice free from parasitic infections. They were aged 4-6 weeks and weighed 20–25 g. The mice were maintained under conventional conditions of feeding and housing in the biological unit of Theodor Bilharz Research Institute (TBRI). They were housed at a room temperature of 20-22^{O}C and kept for a week before the experiment to adapt to the laboratory environment (Ridley and Hawgood, 1956).

Ethical considerations: Animals handling in the current experimental study were done according to the ethical and technical regulations and according to internationally valid guidelines and approved by an institution responsible for animal ethics at October 6 University (O6U) (approval number PME-Me-2201011).

Immunosuppression: All mice were immunosuppressed by oral gavage of dexamethasone (Dexazone tablets 0.5 mg, Al Kahira Pharmaceutical and Chemical Industries Company, Egypt) at a dose of 0.25µg/gm/ day for 14 successive days before oral inoculation with *C. parvum* oocysts and continued receiving dexamethasone on alternative days to maintain the mice immunosuppressed after inoculation till the time of sacrification (Tarazona *et al.,* 1998).

Animal infection:Mice in different study groups were infected by oral gavage with genetically verified *C. parvum* oocysts provided by TBRI in a dose of 3 x 10^3 oocysts dissolved in 200 µL PBS (Gaafar, 2007; Benamrouz *et al*., 2012); then fecal pellets were collected daily post-infection (PI) to be subjected to parasitological examination using Kinyoun's Acid-Fast stain to detect oocysts for confirmation of infection, and then the treatment program started. Oocyst shedding started on the 2nd day PI in all infected immunosuppressed groups and reached its peak on 7th days PI (Moawad *et al*., 2021).

Study design: Immunosuppressed mice were divided into three main groups; these groups were divided into subgroups; each subgroup contained eight mice, as follows: GIA: non-infected mice (negative control); GIB: infected non-treated mice (positive control); GII: infected mice rece-ived CS NPs; GIIIA: infected mice receiving NTZ; GIIIB: infected mice received *Artemisia absinthium* (AA) and *Curcuma longa* (CL)

loaded on CS NPs; GIIIC: infected mice received NTZ conjugated with AA and CL loaded on CS NPs; GIIID: infected mice received combined unloaded free AA and CL.

Therapeutic preparations: 1- Nitazoxanide® (NTZ): NTZ (Nanazoxid, Medizen Pharmaceutical Industries for Utopia Pharmaceuticals) was given according to Li *et al*. (2003). 2- *Artemisia ab-sinthium* (AA): Artemether (Artemidine®, Kunming Pharmaceutical Cooperation, People's Rep-blic of China) was given (Fayer and Ellis, 1994). 3- *Curcuma longa* (CL): Curcumin powder (*C. longa* C1386, Sigma-Aldrich, USA) was given (Henin, 2022). 4- Chitosan nanoparticles (CS NPs): Chitosan (Sigma-Aldrich, USA) was given (Etewa *et al*, 2018). The synthesis procedure and loading of CS NPs with AA and CL were carried out according to the ionotropic gelation technique (Ohya *et al*, 1994).

According to the experimental design, different therapeutic preparations were given to the animals in GII and III on 7^{th} day post-infection (PI) for seven consecutive days.

Parasitological assessment: Fresh fecal pellets from each infected mouse in the study groups were collected on the 7^{th} &14^{th} days of PI, stained by Kinyoun's acid-fast stain (cold method), and examined microscopically to count the number of *C. parvum* oocyst shedding. The oocyst number was calculated per gram of feces (Atia *et al*, 2021). The percentage reduction (efficacy of therapeutic preparations) was then calculated using the formula of Hosking *et al*. (1996).

Histo-pathological examination: Specimens from the small intestine, liver, lung, and kidney were immediately collected after mice scarification, preserved, and manipulated according to Moawad *et al*. (2021) to identify pathological changes in hematoxylin and eosin (H&E) tissue sections as well as to assess the effect of AA and CL, CS NPs, and NTZ on different regimens according their groups.

Determination of oxidative stress markers**:**

Toxicity was determined in serum and different tissues (intestine and liver) of all studied groups by measurement of glutathione (GSH) and lipid peroxide (malondialdehyde) (MDA) using colorimetric methods (Chakraborty *et al*, 2011).

Statistical analysis: Data was collected and subjected to statistical analysis using SPSS (version 16.0). Numerical data was expressed as mean and standard deviation (± SD). The independent simple t-test was used to identify the statistical significance of the difference between the control group and each treated group. A one-way analysis of variance (ANOVA) test was used to identify the statistical significance differences between more than two study group means, and the post hoc test (Tukey HSD) was used to identify the statistical significance of the difference between groups. P-value was considered non-significant at level of $p > 0.05$, significant at level of $p< 0.05$, highly significant at level of $P< 0.01$, and very highly significant at level of $P< 0.001$ (Peat and Barton, 2005).

Results

Shedding of *C. parvum* oocysts started on the 2^{nd} day post-infection (PI) in all immuno-suppressed infected mice with a peak reached on the 7th day PI. The parasitological examination of one gram of stool revealed a significant reduction ($p<0.001$) of *C. parvum* oocyst in GIIID in comparison to all treated groups, as the mean percentage reduction was 88%, followed by GIIIB showed 74%. GIIIC and GIIIA mean reductions were 62% & 44%, respectively, while GII was 20%.

Histopathological examination: Intestine, liver, lung, and renal tissues in GIIID showed a nearly normal pattern and architecture more in the intestinal tissue sections. But, GIIIA received conventional NTZ showed mild histopathological improvement.

Oxidative stress markers (GSH & MDA) levels in serum and different organs (intestine & liver) showed a high significant improvement ($P< 0.001$) in GIIID versus other

groups treated with their levels near GIA.

Details were in table (1) and figures (1, 2, 3, 4, 5, 6, 7, 8 & 9).

Table 1: Comparison between immunosuppressed infected mice in shedding of *C. parvum* oocyst in a gram of stool and reduction % (efficacy %).

Variations		Negative control	Infected treated groups				
		GIB	GII	GIIIA	GIIIB	GIIIC	GIIID
M±SD		273.4±4.7	219.6±7.8	152.2±6.6	72.4± 3.4	103.6±4.9	33.6±5.5
Efficacy %		-	20%	44%	74%	62%	88%
P. value		-	0.001**	0.001**	0.001**	0.001**	0.001**
ANOVA (F-test)		b P. value = 0.001**					
Post-Hoc test Tukey HSD b P. value	GIB	-	0.001**	0.001**	0.001**	0.001**	0.001**
	GII	-	-	-	0.001**	0.001**	0.001**
	GIIIA	-	-	-	-	0.001**	0.001**
	GIIIB	-	-	-	-	0.001**	0.001**
	GIIIC	-	-	-	-	-	0.001**

** Initial p value < 0.001 very highly significant.

Discussion

Nitazoxanide is considered the drug of choice approved by the FDA in treatment of immunocompetent individuals infected with the coccidian intestinal parasite *Cryptosporidium parvum*, but it was not proved as effective as in immunosuppressed individuals with a fatal prognosis (Moawad *et al*, 2021). Therefore, this study aimed to assess the efficacy of the *Artemisia absinthium* (AA) and *Curcuma longa* (CL) combination unloaded or loaded on chitosan nanoparticles (CS NPs) and conjugated with the conventional nitazoxanide (NTZ) in treating cryptosporidiosis in dexamethasone immunosuppressed murine model.

In the present study, shedding of *C. parvum* oocyst started on the 2nd day post-infection (PI) all the infected immunosuppressed groups and reached its peak on 7th day (PI). This agreed with El-Wakil *et al*. (2021). The lowest shedding of *C. parvum* oocyst was observed in GIIID (received AA & CL free combination), with the highest mean efficacy of 88%, followed by GIIIB (received AA & CL loaded on CS NPs), and GIIIC, which received the same combination conjugated with NTZ and loaded on CS NPs were74% and 62%, respectively. GIIIA, receiving the conventional free NTZ, showed an efficacy of only 44%.

This agreed with El-Wakil *et al*. (2021), who reported that NTZ was not effective in improving cryptosporidiosis diarrhea or mortality rates in immunosuppressed mice. A Also, Li *et al*. (2003) recorded that NTZ reduced the oocyst shedding in infected immunosuppressed mice, with a relatively higher mean reduction of about 50% versus 44% of the current work, however still significantly less than the results of the AA and CL free combination in this present (88%). However, El-Ashkar *et al*. (2022) reported the effect of NTZ, Ivermectin, and Artemether (ART) against cryptosporidiosis in immunosuppressed diabetic mice. They found the best result in ART-treated group, with a mean reduction in oocyst shedding of about 88.58% which is near to the present data using AA combined with CL. Formerly, ART, the approved antimalarial derived from *Artemisia,* was used to suppress *Cryptosporidium* growth in cell culture (Wu *et al*, 2011). When anti-malarial mefloquine (MQ) as compared with NTZ in same animal model, oocyst showed clearance (100% &53%, respectively) when given on 14th day PI (El-Wakil *et al*, 2021).

In the present study, when AA and CL combination was loaded on CS NPs (GIIIB) showed a reduction efficacy of 74%. This agreed with Said *et al*. (2012), who studied the CL with CS NPs effect on *Giardia lamblia* found a mean cyst reduction of 64.4%. They also studied the effect of CS NPs and Ag NPs with CL NPs against *G. lamblia* and found that less effect as a mean cyst reduction of CS NPs than Ag NPs was 83.1 versus 87.2%, respectively.

Teimouri *et al*. (2018) reported convenient

results with the same present carrier nanopa rticles, but with different molecular weights in case of the tissue *Toxoplasma gondii*, that the effect of CS NPs in the infected immunosuppressed mice showed growth inhibition rates of tachyzoites in peritoneal exudates of mice receiving low, medium, and high molecular weights of CS NPs to be 86%, 84% and 79% respectively. The present work disagreed with these authors for CS NPs in GII infected with *C. parvum* showed 20% efficacy of oocysts reduction.

In the present work H&E sections of small intestine in positive control showed a profound effect on the intestinal mucosa structure as compared to negative control. This was a decrease in the villous-to-crypt ratio, villous expansion, tip region erosions, and goblet cell depletion. This more or less agreed with Hassan *et al*. (2021), who reported pathological changes in both immunocompetent and immunosuppressed individuals, including shortening and broadening of villi, loss of villous architecture with a decreased ratio of villous height to crypt length, and goblet cell depletion, which were more severe in immunosuppressed ones.

In the present work, the small intestine section of GIIID (received AA & CL free combination) showed obvious improvement in the form of villi pattern back to normal, with average length, width, goblet cell number, and conventional pattern of inflammatory cells. GIIIB (received AA & CL loaded on CS NPs) and GIIIC received the same combination, but conjugated with NTZ showed only partial amelioration mild decrease in the villous to crypt ratio, with mild villous expansion, mild inflammatory cellular infiltration, and goblet cell regeneration. But, histopathological changes showed mild or no improvement in GII (CS NPs) and GIIIA (NTZ), by decrease in villous to crypt ratio, with villous expansion by inflammatory cells and goblet cell depletion.

The CS NPs effect on intestine was reported by Moawad *et al*. (2021), who reported the presence of *C. parvum* at the enterocytes brush border with moderate infiltration of inflammatory cells and superficial ulceration. The NTZ effect was reported by Hassan *et al*. (2021), who found that NTZ alone was not efficient in treating immunosuppressed cryptosporidiosis. Previously, Ramírez-Tortosa *et al*. (1999) reported that the CL pharmaco-dynamical distribution when given orally was significant since 35% of the CL remained in the intestinal tract and passed with feces, with effectiveness intestinal protozoa elimination.

In the current work, liver tissue sections of negative control showed normal hepatic lobular architecture, but positive control showed patchy hepatocellular hydropic degeneration and a focal intra-lobular aggregate of neutrophils due to extra-intestinal spreading. A marked reduction of hepatic tissue pathology appeared in GIIID (free combination of AA & CL), which showed only focal intralobular aggregate of neutrophils without hepatocellular hydropic degeneration. GIIIA (NTZ) showed partial improvement with patchy hepatocellular hydropic degeneration. But, Mohamed *et al*. (2019) in 14 days study found liver changes in NTZ treated immunosuppressed mice as intact lobular hepatic architecture with thin normal hepatocytes plates, congested central vein, interlobular lymphocytes in small collection and congested dilated sinusoids. No doubt, more duration allowed drug in ameliorating extra-intestinal cryptosporidiosis spreading.

In the present work, GII received only CS NPs or GIIIB & IIIC loaded on CS NPs didn't show hepatic improvement as liver sections showed patchy hepatocellular hydropic degeneration and necrosis denoting that CS NPS carrier molecules not allowed the recovery. Moawad *et al*. (2021) found that the CS NPs on liver tissue in immunosuppressed cryptosporidiosis infected mice with moderate inflammatory infiltrate, binucleated cells (large dysplastic cells), and vacuolar degeneration.

In the present study, lung and renal tissues showed marked amelioration of pathological

changes only in GIIID given combination of natural herbs; AA & CL, but others showed mild to moderate lung and renal tissues pathology. Madbouly *et al*. (2017) reported that changes in lung tissue of infected immunosuppressed mice treated with a combination of NTZ and atorvastatin caused pulmonary hemorrhage and interstitial inflammations.

In the present work, glutathione (GSH) and malondialdehyde (MDA) was measured as toxic markers in serum, intestine, and liver in all groups. Serum and tissue (intestine and liver) GSH levels were mostly improved in GIIID given free combination of the natural herbs; AA & CL, followed by NTZ-treated (GIIIA). The least value was in serum and liver of GIIIB, where AA and CL were loaded on CS NPs, but toxicity was more in intestine in mice received only CS NPs. Chakraborty *et al*. (2011) measured CS NPs toxicity in serum and organs of infected-treated mice, reported that chitosan nanoparticles modified with folate improved antioxidative effect.

In the present work, MDA levels (serum and tissue) showed least toxicity was less in GIIID received only combined AA & CL herbal preparations. This agreed with Mohamed *et al*. (2019), who reported in immunocompetent and immunosuppressed cryptosporidiosis infected mice, MDA levels decreased in all treated groups as compared to positive control. Also, the present study showed that more toxicity MDA levels were in GIIIB & IIIC, given therapeutic loaded on CS NPs. Mohamed *et al*. (2019), who found the highest reduction in MDA hepatic levels in mice treated with *Nigella* loaded on CS NPs. Also, Mo *et al*. (2022) reported that the MDA hepatic levels improved hepato-renal toxicity in rats given carbendazim® loaded on newly synthesized CS NPs rather than unloaded one.

Conclusion

Combined *Artemisia absinthium* and *Curcuma longa,* preferably unloaded on CS NPs and unconjugated with NTZ proved to be effective and safe in treating experimental intestinal cryptosporidiosis in immunosuppressed mice. Thus, it is very promising to try or to repurpose in immunocompromised human cases; however, their use in cases of extra-intestinal organ involvement is recommended for a longer period.

Conflicts of interest: Authors declared that they neither have conflict of interest nor received any funds. Also, they equally shared in all the theoretical and practical parts, and shared in writing, and revising the manuscript and approved its publication.

References

Asadpour, M, Namazi, F, Razavi, SM, Nazifi, S, 2018: Comparative efficacy of curcumin and paromomycin against *Cryptosporidium parvum* infection in a BALB/c model. J. Vet. Parasitol. 250:7-14.

Atia, AF, EL Sobky, MM, Harba, NM, Elmehy, RA, Allam, DM, *et al,* 2021: Evaluation of potential prophylactic and therapeutic effect of azoximer bromide (polyoxoanion) on experimental cryptosporidiosis in the immunocompromised mice. JPU 14, 3:293-304.

Benamrouz, S, Guyot, K, Gazzola, S, Mouray, A, Chassat, T, *et al*, 2012: *Cryptosporidium parvum* infection in SCID mice infected with only one oocyst: qPCR assessment of parasite replication in tissues and development of digestive cancer. J. PLoS One 7, 12:1- 7.

Beshay, J, 2018: Therapeutic efficacy of *Artemisia absinthium* against *Hymenolepis nana*: In vi-0tro and in vivo studies in comparison with the anthelminthic praziquantel. J. Helminthol. 92, 3: 298-308.

Bouzid, M, Kintz, E, Hunter, PR, 2018: Risk factors for *Cryptosporidium* infection in low- and middle-income countries: A systematic review and meta-analysis. J. PLoS Negl. Trop. Dis. 12, 6:e0006553.

Breurec, S, Vanel, N, Bata, P, Chartier, L, Farra, A, *et al*, 2016: Etiology and epidemiology of diarrhea in hospitalized children from low-income country: A matched case-control study in Central African Republic. J. PLoS Negl. Trop. Dis. 10:e0004283.

Caner, A, Döşkaya, M, Değirmenci, A, Can, H, Baykan, S, *et al*, 2008: Comparison of the effects of *Artemisia vulgaris* and *Artemisia absinthium* growing in western Anatolia against trichinellosis (*Trichinella spiralis*) in rats. J. Exp.

Parasitol. 119: 173-9.
Chakraborty, SP, Mahapatra, SK, Sahu, SK, Pramanik, P, Roy, S, 2011: Anti-oxidative effect of folate-modified chitosan nanoparticles. Asian Pac. J. Trop. Biomed. 1, 1:29-38.
Checkley, W, White, AC, Jaganath, D, Arrowood, MJ, Chalmers, RM, *et al*, 2015: A review of the global burden, novel diagnostics, therapeutics, and vaccine targets for *Cryptosporidium*. J. Lancet Infect. Dis. 15, 1:85-94.
De Jong, WH, Borm, PJ, 2008: Drug delivery and nanoparticles: Applications and hazards. Int. J. Nanomed. 3, 2:133-49.
Ekiert, H, Świątkowska, J, Klin, P, Rzepiela, A, Szopa, A, 2021: *Artemisia annua*: Importance in traditional medicine and current state of knowledge on chemistry, biological activity and possible applications. J. Planta Med. 87, 8:584-99.
El-Ashkar, AM, Mahmoud, S, Sabry, H, Guirguis, N, El Komi, W, *et al*, 2022: Nitazoxanide, Ivermectin, Artemether effect against cryptosporidiosis in diabetic mice: Parasitological, histopathological, and chemical studies. J. Parasit. Dis. 46, 4:1070-9.
El-Wakil, ES, Salem, AE, Al-Ghandour, A, 2021: Evaluation of possible prophylactic and therapeutic effect of mefloquine on experimental cryptosporidiosis in immunocompromised mice. J. Parasit. Dis. 45:380-93.
Etewa, SE, Abo El-Maaty, DA, Hamza, RS, Ashraf, S, Metwaly, AS, *et al*, 2018: Assessment of spiramycin-loaded chitosan nanoparticles treatment on acute and chronic toxoplasmosis in mice. J. Parasit. Dis. 42, 1:102-13.
Fayer, R, Ellis, W, 1994: Qinghaosu (artemisinin) & derivatives fail to protect neonatal BALB /c mice against *Cryptosporidium parvum* (*Cp*) infection. J. Eukaryote Microbiol. 41, 5: S 41.
Ferreira, JF, Peaden, P, Keiser, J, 2011: In vitro trematocidal effects of crude alcoholic extracts of *Artemisia annua, A. absinthium, Asimina triloba*, and *Fumaria officinalis*: Trematocidal plant alcoholic extracts. J. Parasitol. Res. 109, 6:1585-92.
Gaafar, MR, 2007: Effect of solar disinfection on viability of intestinal protozoa in drinking water. J. Egypt. Soc. Parasitol. 37, 1:6586.
Hassan, ZR, Osman, FH, Shalash, IR, Magdy, M, Abd Rabbo, M, 2021: Effect of silver nanoparticles loaded nitazoxanide in treatment of murine cryptosporidiosis in immunocompetent and immuno-suppressed mice. Al-Azhar Uni. J. Res. Stud. 3, 1:1-15.
Henin, RW, 2022: Effect of some medicinal herbs versus nitazoxanide on *Cryptosporidium parvum* infected immunosuppressed mice. JESP 52, 3:395-402.
Hosking, BC, Watson, TG, Leathwick, DM, 1996: Multigeneric resistance to oxfendazole by nematodes in cattle. Vet. Rec. 138, 3:67-8.
Khater, MM, El-Sayed, SH, Yousof, HAS, Mahmoud, SS, El-Dib, N, *et al,* 2017: Anti-*Cryptosporidium* efficacy of *Olea europaea* and *Actinidia deliciosa* in neonatal mouse model. Kasr El Aini Med. J. 23, 1:32-7.
Li, X, Brasseur, P, Agnamey, P, Lemeteil, D, Favennec, L, *et al,* 2003: Long-lasting anti-cryptosporidial activity of nitazoxanide in an immunosuppressed rat model. J. Folia Parasitol. 50, 1:19-22.
Madbouly, NT, Hebat, SA, Yousof, HA, El-Sayed, SH, Younis, AI, *et al,* 2017: Atorvastatin repurposing for the treatment of cryptosporidiosis in experimentally immunosuppressed mice. Exp. Parasitol. 181: 57-69
McCole, DF, Eckmann, L, Laurent, F, Kagnoff, MF, 2000: Intestinal epithelial cell apoptosis following *Cryptosporidium parvum* infection. J. Infect. Immune 68, 3:1710-3.
Mo, E, Ebedy, YA, Ibrahim, MA, Farroh, KY, Hassanen, EI, 2022: Newly synthesized chitosan-nanoparticles attenuate carbendazim hepatorenal toxicity in rats via activation of Nrf2/HO1 signaling pathway. J. Sci. Reports 12, 1:9986.
Moawad, H, Hegab, M, Badawey, M, Ashoush, S, Ibrahim, S, *et al,* 2021: Assessment of chitosan nanoparticles in improving the efficacy of nitazoxanide on cryptosporidiosis in immunosuppressed and immunocompetent murine models. J. Parasit. Dis. 45, 3:606-19.
Mohamed, WA, Koura, EA, Rabee, I, Hammam, OA, Ismail, HM, 2019: Efficacy of chitosan nanoparticle alone versus conjugated with *Nigella sativa* (EL Baraka seed oil) against *Cryptosporidium parvum* in infected immunocompetent and immunosuppressed mice. J. Pharma. Pharm. Sci. 8, 10:139-61.
Nanjwade, BK, Bellad, KA, Mohamied, AS, Nwaji, MS, Srichana, T, 2015: Curcumin: Nutraceutical and pharmaceutical applications. J. Adv. Pharmacog. Phytomed. 1, 1:17-26.
Ohya, Y, Shiratani, M, Kobayashi, H, Ouchi, T, 1994: Release behavior of 5-Fluorouracil from chitosan-gel nanospheres immobilizing 5-Fluorouracil coated with polysaccharides and

their cell specific cytotoxicity. J. Macromol. Sci. A. 31, 5:629-42.

Padosch, SA, Lachenmeier, DW, Kröner, LU, 2006: Absinthium: A fictitious 19th Century syndrome with present impact. J. Subst. Abuse Treat. Prevent. Policy 1:1-14.

Peat, J, Barton, B, 2005: Medical statistics: A guide to data analysis and critical appraisal. First Ed.: Wiley-Blackwell.

Ramírez-Tortosa, MC, Mesa MD, Aguilera M C, Quiles JL, Baró L, *et al,* 1999: Oral administration of a turmeric extract inhibits LDL oxidation and has hypocholesterolemia effects in rabbits with experimental atherosclerosis. J. Atherosclerosis 147, 2:371-8.

Ridley, DS, Hawgood, BC, 1956: Value of formol-ether concentration of fecal cysts and ova. J. Clin. Pathol. 9:74-6

Said, D, Elsamad, L, Gohar, Y, 2012: Validity of silver, chitosan, and curcumin nanoparticles; as anti-*Giardia* agents. J. Parasitol. Res. 111, 2: 545-54.

Soufy, H, El-Beih, N, Nasr, S, El-Aziz, T, Khalil, F, *et al,* 2017: Effect of Egyptian propolis on cryptosporidiosis in immunosuppressed rats with special emphasis on oocysts shedding, leukogram, protein-profile and ileum histopathology. Asian Pac. J. Trop. Med. 10, 3:253-62.

Tarazona, R, David, A, Belwett, N, Manuel, S, Carmona, MD, 1998: *C. parvum* infection in experimentally infected mice: Infection dynamics and effect of immunosuppression. Folia Parasitol. 45, 2:101-7.

Teimouri, A, Azami, SJ, Keshavarz, H, Esmaeili, F, Alimi, R, *et al,* 2018: Anti-*Toxoplasma* activity of various molecular weights and concentrations of chitosan nanoparticles on tachyzoites of RH strain. Int. J. Nanomed. 13:1341-51.

Yanat, M, Schroen, K, 2021: Preparation methods and applications of chitosan nanoparticles with an outlook toward reinforcement of biodegradable packaging. J. React. Funct. Polymers 161:1-12.

Wu, L, Jiang, X, Shen, Y, Lu, Z, Tu, G, *et al,* 2011: Efficacy of ginkgolic acids against *Cryptosporidium andersoni* in cell culture. Parasitol. Res. 109:1475-9.

Explanation of figures

Fig. 1: Small intestine section stained with H&E: A- GIA (200X) showed regular villous pattern in length (orange line) and width (yellow line) with average number of goblet cells (black arrows) and mild inflammatory cells (blue arrow). B- GIB (200X) showed decrease in villous to crypt ratio (orange to yellow lines), with villous expansion (green line), tip region erosions (black arrows) and goblet cell depletion (blue arrows). C- GII (400X) showed decrease in villous to crypt ratio (orange to yellow lines), with villous expansion by inflammatory cells (red arrow) and goblet cell depletion (blue arrows). D- GIIIA (200X) showed short villi, with villous expansion (yellow line) by inflammatory cell (black arrow), and goblet cell depletion (blue arrows). E GIIIB (200X) showed mild decrease in villous to crypt ratio (orange to yellow lines), with mild villous expansion (green line), mild inflammatory cellular infiltration and goblet cell regeneration (black arrows). F- GIIIC (200X) showed regenerated villi (blue lines) with focal tip region erosions (black arrows) and goblet cell regeneration. G- GIIID (400X) showed a nearly normal pattern of villi with average length, width, goblet cell number and inflammatory cells conventional pattern

Fig. 2: H&E stained section of liver tissue shows: A- GIA (200X) showed normal hepatic lobular architecture. B- GIB (200X) showed patchy hepatocellular hydropic degeneration (black arrow) and focal intralobular aggregate of neutrophils (red arrow). C- GII (400X) section showed patchy hepatocellular hydropic degeneration (red arrow) and focal intralobular aggregate of neutrophils (black arrow). D- GIIIA (400X) showed patchy hepatocellular hydropic degeneration (red arrows). E- GIIIB (400X) showed patchy hepatocellular hydropic degeneration (blue arrow), focal intralobular aggregate of neutrophils (yellow arrow) and necrosis. F- GIIIC (400X) showed focal intralobular aggregate of neutrophils (yellow arrow) & necrosis (red arrow). G- GIIID (200X) showed focal intralobular aggregate of neutrophils (yellow arrow) without hepat-ocellular hydropic degeneration.

Fig. 3: Lung tissue stained with H&E stained: A- GIA (200X) showed normal architecture with thin-walled alveoli (red arrow), small bronchioles (black arrow) and delicate blood vessel. B- GIB (200X) showed collapsed alveoli infiltrated by some lymphocytes (red arrow) and mild hyperplasia of bronchiolar epithelium (black arrow) and mildly thickened blood vessel. C- GII (200X) showed collapsed alveoli infiltrated by some lymphocytes (red arrow) and moderate hyperplasia of bronchiolar epithelium (black arrows). D- GIIIA (200X) showed collapsed alveoli infiltrated by some lymphocytes (red arrow) and bronchiolar epithelium moderate hyperplasia (black arrows). E- GIIIB (400X) showed collapsed alveoli (yellow arrow), infiltrated by some lymphocytes (red arrow) and focal ulceration of bronchiolar epithelium (black arrows). F- GIIIC (400X) showed collapsed alveoli infiltrated by some lymphocytes (red arrow) and marked hyperplasia of bronchiolar epithelium (black arrows). G- GIIID (400X) showed normal alveoli with focal peri-bronchial infiltration by lymphocytes (red arrow) and moderate hyperplasia of bronchiolar epithelium (black arrows).

Fig. 4: Mean serum glutathione (GSH) levels in uninfected and infected immunosuppressed untreated and treated mice.

Fig. 5: GSH levels in uninfected and infected immunosuppressed untreated and treated mice.

Fig. 6: GSH levels in uninfected and infected immunosuppressed untreated and treated mice.

Fig. 7: Mean serum malondialdehyde (MDA) levels in uninfected and infected immunosuppressed untreated and treated mice.

Fig. 8: MDA levels in uninfected and infected immunosuppressed untreated and treated mice.

Fig. 9: MDA levels in uninfected and infected immunosuppressed untreated and treated mice.

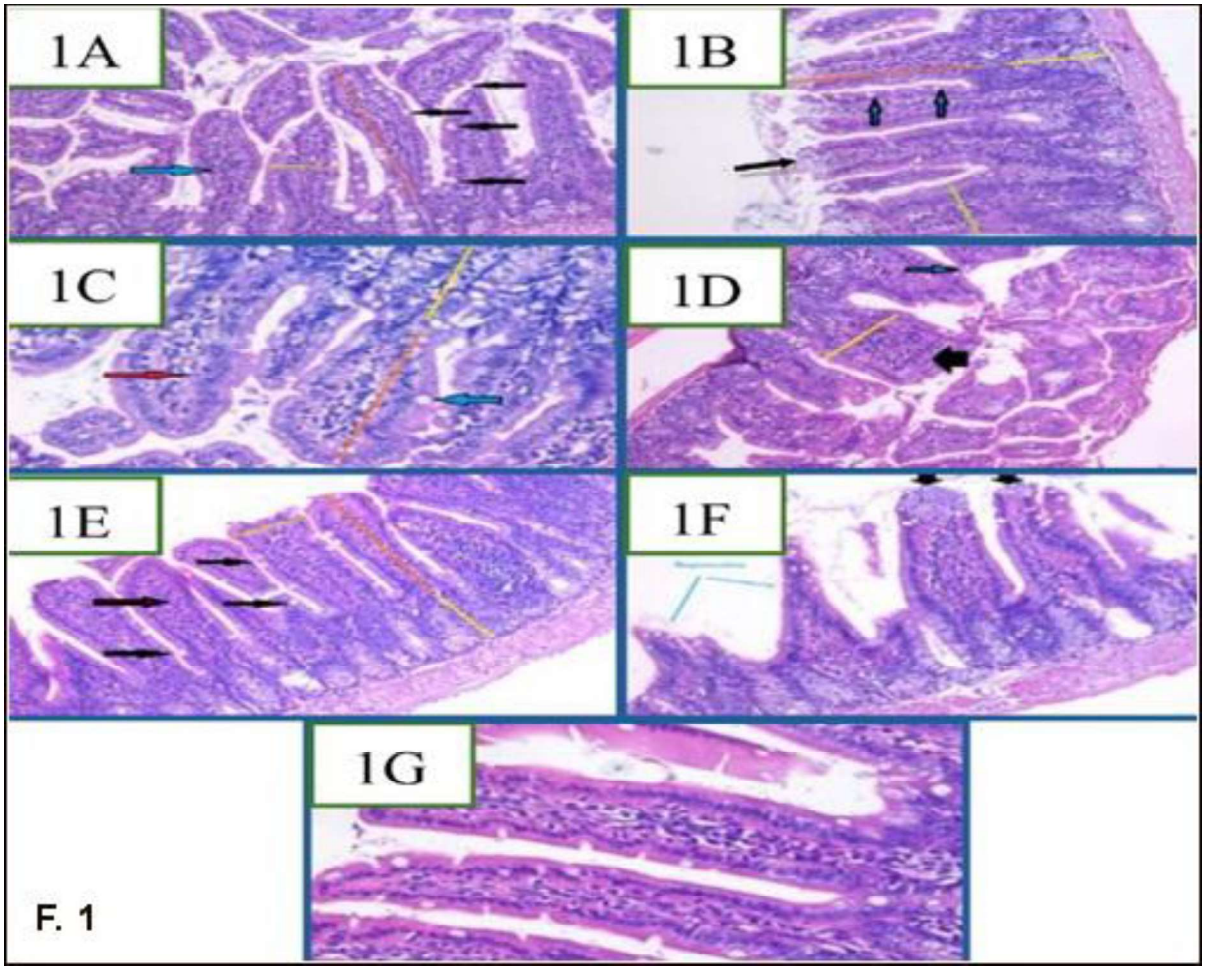

F. 1

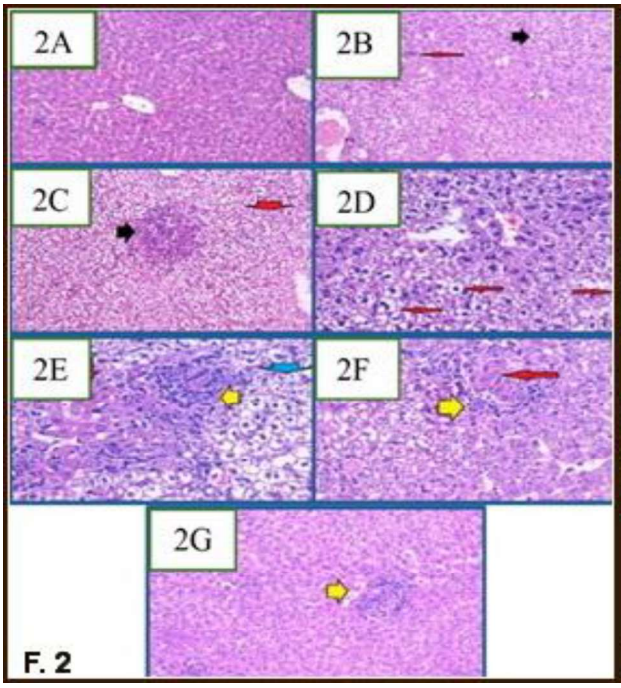

F. 2

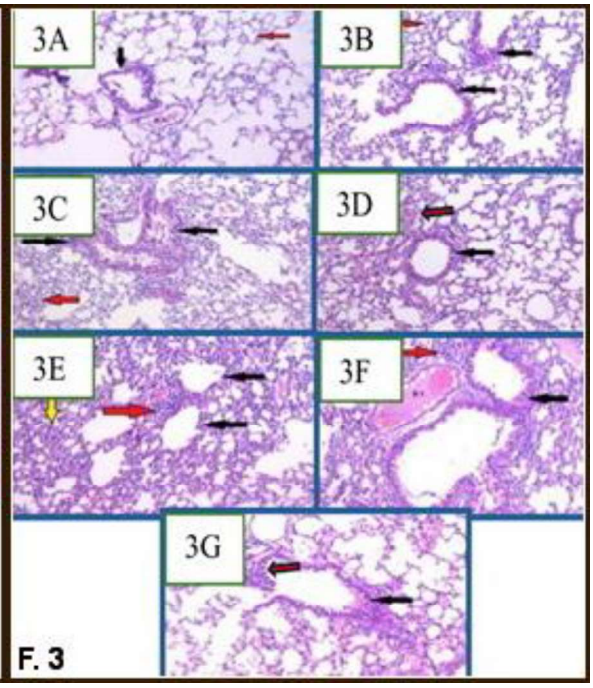

F. 3

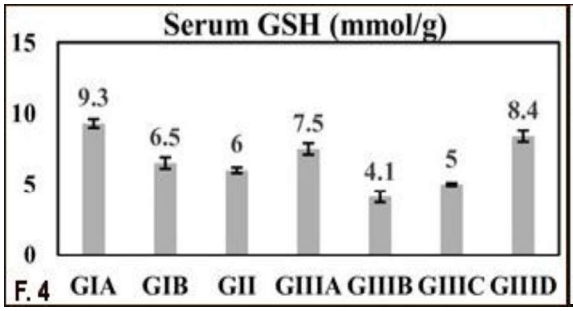

F. 4

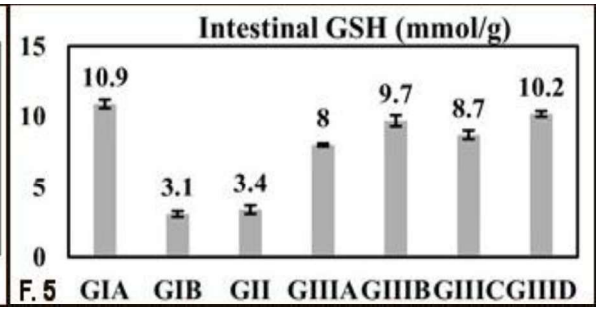

F. 5

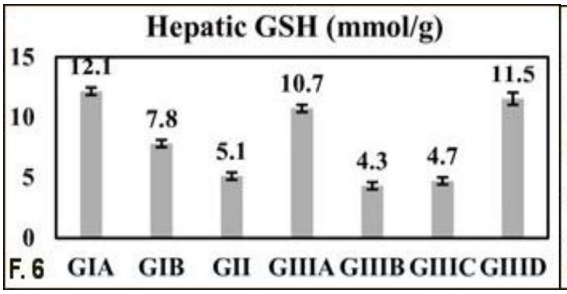

F. 6

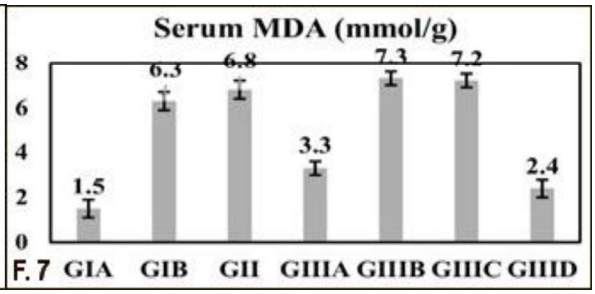

F. 7

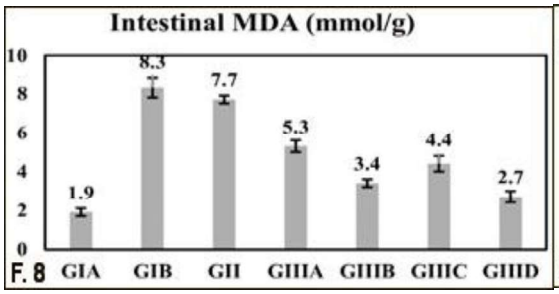

F. 8

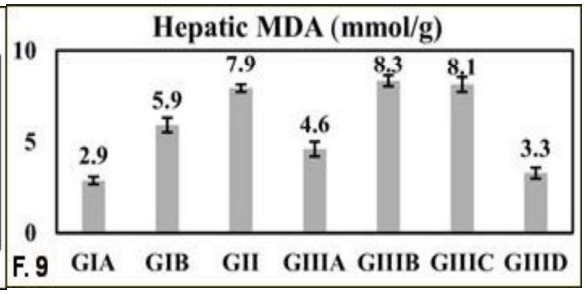

F. 9